Condensed Matter Physics, 1999, Vol. 2, No. 1(17), p. 155–171

CONDENSED MATTER PHYSICS

Configurational splitting in Raman scattering spectra of crystals with the order-disorder type phase transitions

I.V.Stasyuk, Ya.L.Ivankiv

Institute for Condensed Matter Physics
of the National Academy of Sciences of Ukraine,
1 Svientsitskii Str., 290011 Lviv, Ukraine

Received June 23, 1997

A system of equations for the averaged phonon Green function determining the shapes of the lines in Raman scattering spectra is obtained in the coherent potential approximation. Configurationally split components of the Raman scattering are studied within a simple model. For the KH_2PO_4 and the CsH_2PO_4-type ferroelectrics the possibility to observe the configurational splitting experimentally is discussed.

Key words: *Raman scattering, configurational splitting, order-disorder type phase transitions, ferroelectrics*

PACS: *77.84.Fa, 78.30.Ly*

1. Introduction

A study of spectra of the Raman scattering of light in KH_2PO_4 (KDP) crystals is of specific interest for the discussion of phase transitions in these systems. Developments in the dynamical theory of phase transitions in KDP crystals have made the concept of a proton-phonon soft mode widely used.

A frequency range related to phase transitions has become a subject of many investigations [1,2], because low-frequency lattice modes are most closely related to transition phenomena. Besides, it is of interest to study phonon modes at even higher frequencies, in particular those which are related to the internal oscillations of phonon groups. In crystals with order-disorder transitions, the specific features of these oscillations depend on the states or orientations of the structure elements that are ordered (the ionic groups and protons on hydrogen bonds). A new model for phase transitions in KDP crystals has been proposed [3-7] on the basis of the experimental data for ν_3 and ν_4 modes in scattering geometries for which the observation of such modes is forbidden by the selection rules for site symmetry S_4 [8]. The model assumes that the main role in the transition belongs to the ordering

© I.V.Stasyuk, Ya.L.Ivankiv

of PO_4 dipoles which already existed in a high temperature phase rather than to the ordering of protons on H-bonds, i.e. the softening of a related proton-phonon mode. However, the application of the model encounters difficulties because the "ice" rule (one proton on bond and two protons close to the PO_4 group) is violated.

On the other hand, the idea about H_2PO_4 groups ordering is not confirmed by the NMR experimental data for KH_2PO_4 [9]. Thus, a clear interpretation of the available data has not been achieved. The results obtained can be explained satisfactorily even within the framework of the proton ordering model. It was shown in [10] that the description of the Raman spectra of internal oscillations in KH_2PO_4 clusters can be made if different realizations of proton configurations are taken into account. The model can easily be extended to allow for the short-range proton correlations [11].

In this respect it is interesting to study the peculiarities of phonon spectra of KDP crystals in more detail. In particular, the functions of spectral densities which determine the shape of lines in the Raman spectra are of importance. The subject of our study are the crystals in which phase transitions are related to the ordering of protons in one-dimensional chain structures.

2. A system of equations for the averaged Green function. Coherent potential approximation

An effective cross-section which is the main characteristic of the Raman scattering can be expressed as [12,13]

$$\frac{\mathrm{d}^2\sigma}{\mathrm{d}\Omega d\omega_2} = \frac{1}{(4\pi\varepsilon_0)^2}\sqrt{\frac{\varepsilon_2}{\varepsilon_1}}\frac{\omega_2^3\omega_1}{\hbar^2c^4}\sum_{\substack{\alpha\beta\\ \alpha'\beta'}} e_{1\alpha}e_{2\beta}e_{1\alpha'}e_{2\beta'} \tag{2.1}$$

$$\times\frac{1}{2\pi}\int\limits_{-\infty}^{+\infty}\mathrm{d}t\ \mathrm{e}^{i(\omega_1-\omega_2)t}\langle\hat{P}^{\beta'\alpha'}_{\mathbf{k}_2,-\mathbf{k}_1}(-\omega_1,t)\hat{P}^{\beta\alpha}_{-\mathbf{k}_2,\mathbf{k}_1}(\omega_1,0)\rangle,$$

where $\mathbf{e}_1$, $\mathbf{e}_2$ are polarization vectors; ω_1, ω_2 are frequencies and $\mathbf{k}_1$, $\mathbf{k}_2$ are wave vectors of the incident and scattered light, respectively; $\alpha,\beta,\alpha',\beta'$ are coordinate indices; $\varepsilon_{1,2}\equiv\varepsilon(\omega_1,\omega_2)$; $\hat{\mathbf{P}}$ is a polarizability operator:

$$\hat{P}^{\beta'\alpha'}_{\mathbf{k}_2,-\mathbf{k}_1}(-\omega_1,t) = \sum_{nn'}\sum_{ee'}\mathrm{e}^{\mathrm{i}\mathbf{k}_2\mathbf{R}_n}\mathrm{e}^{-\mathrm{i}\mathbf{k}_1\mathbf{R}_{n'}}\hat{P}^{\beta'\alpha'}_{ne,n'e'}(-\omega_1,t), \tag{2.2}$$

(n,n' are cell numbers; l,l' are ion species in the cell)

$$\hat{P}^{\beta'\alpha'}_{ne,n'e'}(-\omega_1,t) = \delta_{nn'}\delta_{ee'}\int\limits_{-\infty}^{+\infty}\mathrm{d}\omega_1'\tilde{P}^{\beta'\alpha'}_{ne}(\omega_1',-\omega_1)\mathrm{e}^{-\mathrm{i}(\omega_1+\omega_1')t}. \tag{2.3}$$

An expression for a scattering cross-section can be written in terms of the Green function constructed by the polarizability operators [10]:

$$\frac{2\pi}{\hbar}\langle\langle \tilde{P}_{l_1}^{\beta\alpha}(\omega_2,\omega_1)|\ \tilde{P}_{l}^{+\beta'\alpha'}(\omega_2,\omega_1)\rangle\rangle_{\omega,\mathbf{q}} = \hbar^2 e^4 \langle \hat{G}_{l_1 l}^{\beta\alpha,\beta'\alpha'}(\omega_2,\omega_1)\rangle_{\omega,\mathbf{q}} \qquad (2.4)$$
$$= \hbar^2 e^4 \sum_{i\varkappa_i}\sum_{j\varkappa_j} \mathbf{R}_{l_1\beta\alpha}^{(j)\varkappa_j}(\omega_2,\omega_1)\ \mathbf{R}_{l\beta'\alpha'}^{*(i)\varkappa_i}(\omega_2,\omega_1)\langle \hat{g}_{l_1 l}^{(ji)\varkappa_j\varkappa_i}(\omega,\mathbf{q})\rangle,$$

where $\mathbf{R}_{l_1\alpha\beta}^{(j)\varkappa_j}(\omega_2,\omega_1)$ is a scattering tensor of the $\varkappa_j$-mode of the l_1-th ion complex having the j-th configuration; $\hat{g}$ is the phonon Green function corresponding to internal vibrations of ion groups.

The Green function $\hat{g}_{l_1 l}^{(ji)\varkappa_j\varkappa_i}$ can be determined from equation [10]:

$$\hat{g} = \hat{\chi} + \hat{\chi}\Phi\hat{g}. \qquad (2.5)$$

Here,

$$\hat{\chi}_{nk}^{(ij)\varkappa_i\varkappa_j} = g_{ok}^{\varkappa_i\varkappa_j}\delta_{ij}\ \hat{B}_{nk}^{ii}$$

is a phonon Green function of an isolated ion complex;

$$g_{0k}^{\varkappa_i\varkappa_j} = \frac{\delta_{\varkappa_i\varkappa_j}}{\omega^2 - \Omega_{k\varkappa_j}^2},$$

$\hat{B}_{nk}^{ii}$ is an occupation number of the i-th configuration of the (n,k)-th complex; Φ is a matrix of interactions between internal vibrations of the complexes.

According to (2.4), the effective cross-section and the Raman scattering tensor are related to the averaged over configurations Green function (2.5). Averages of products of functions $\hat{\chi}$ can be expanded in cumulants. Thence, function $\langle\hat{g}\rangle$ is expressed in terms of full irreducible parts Σ [10]

$$\langle\hat{g}\rangle = (1 - \Sigma\ \Phi)^{-1}\Sigma \qquad (2.6)$$

or

$$\langle g\rangle^{-1} = \Sigma^{-1} - \Phi\ (\mathbf{q}).$$

Certain summation of diagrams for the (self-energy) irreducible part corresponds to equation (2.6). We introduce the diagrammatic notations:

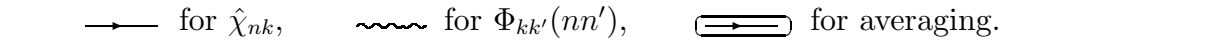

Ovals surrounding n lines correspond to cumulants of the n-th order. An expression for Σ contains only irreducible diagrams (the diagrams which do not break down into separate parts if one interaction line is cut)

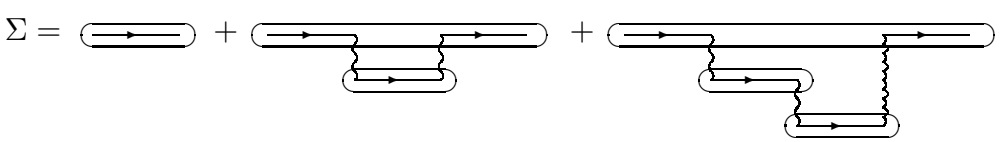

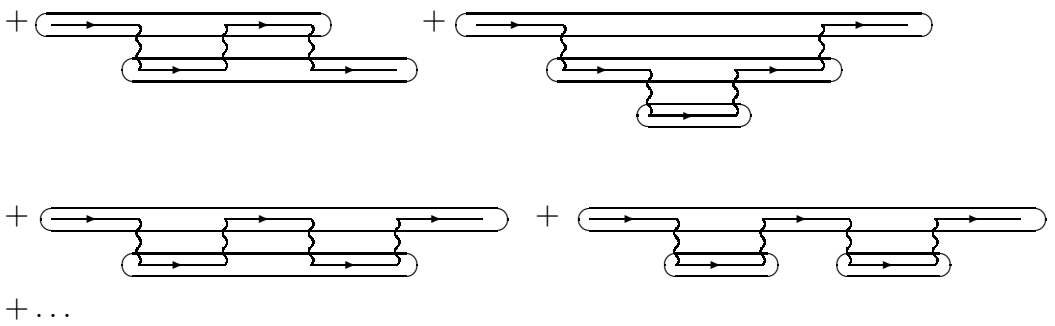

In the spirit of a single-site approximation, the correlation between χ_{nk} is taken into account only if the site indices coincide. Then, we can sum up series (2.6) using a coherent potential approximation. Let us pick in Σ the diagrams the beginnings and ends of which correspond to the same site. In these diagrams, we separate out the ovals corresponding to the same site. As J we denote the sum of diagrams which start and end with lines of interaction on a given site and do not contain ovals with this site. In diagrammatic notations

$J_{kk}(nn)$:

We can calculate $J_{kk}(nn)$ making use of the method described in [14,15]. Hence, we have

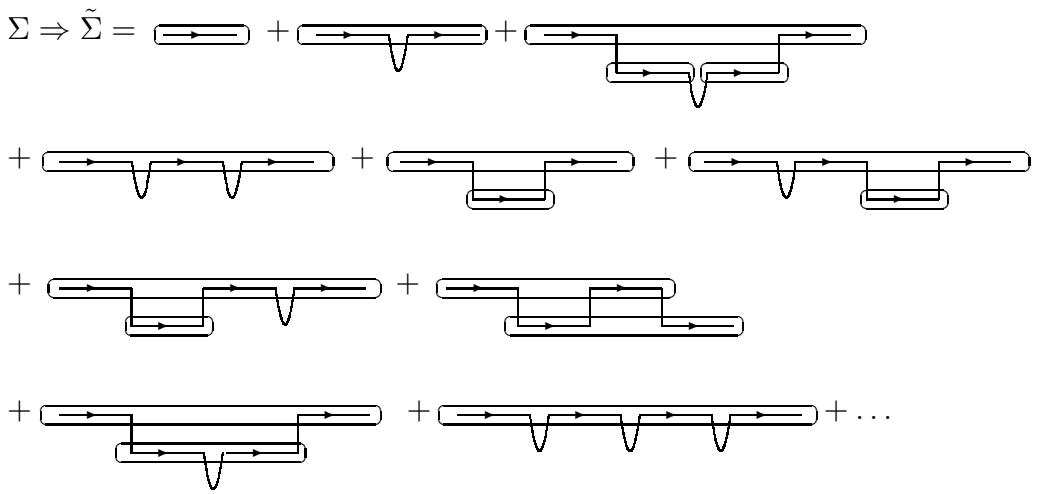

(within J^3).

In a single site approximation we get the following equation for the Green function $\langle\hat{g}_k\rangle$:

$$\begin{aligned}\langle\hat{g}_k\rangle_* &= \tilde{\Sigma}_k + \tilde{\Sigma}_k J_k \tilde{\Sigma}_k + \tilde{\Sigma}_k J_k \tilde{\Sigma}_k J_k \tilde{\Sigma}_k + \cdots \\ &= \tilde{\Sigma}_k + \tilde{\Sigma}_k J_k \langle\hat{g}_k\rangle_*.\end{aligned} \tag{2.7}$$

In this approximation the self-energy part reads

$$\tilde{\Sigma}_k = \langle \hat{g}_k \rangle_* (1 + J_k \langle \hat{g}_k \rangle_*)^{-1}. \tag{2.8}$$

In the calculation of the Green function $\langle \hat{g}_k \rangle$ within a single site approximation, the correlation between unperturbed Green functions of the internal vibrations of the complex (n, k) having the i-th configuration is taken into account only if the site indices coincide. In this case

$$\begin{aligned}
&\langle \hat{g}^{(ij)\varkappa_i\varkappa_j}_{nk,nk} \rangle_* = \\
&= \langle \hat{\chi}^{(ij)\varkappa_i\varkappa_j}_{nk} \rangle + \sum_{\substack{j_1\varkappa_{j_1} \\ j_2\varkappa_{j_2}}} \langle \hat{\chi}^{(ij_2)\varkappa_i\varkappa_{j_2}}_{nk} J^{(j_2j_1)\varkappa_{j_2}\varkappa_{j_1}}_{kk}(nn) \hat{\chi}^{(j_1j)\varkappa_{j_1}\varkappa_j}_{nk} \rangle \\
&+ \sum_{\substack{j_1\varkappa_{j_1} \\ j_2\varkappa_{j_2}}} \sum_{\substack{j_3\varkappa_{j_3} \\ j_4\varkappa_{j_4}}} \langle \hat{\chi}^{(ij_2)\varkappa_i\varkappa_{j_2}}_{nk} J^{(j_2j_1)\varkappa_{j_2}\varkappa_{j_1}}_{kk}(nn) \hat{\chi}^{(j_1j_4)\varkappa_{j_1}\varkappa_{j_4}}_{nk} J^{(j_4j_3)\varkappa_{j_4}\varkappa_{j_3}}_{kk}(nn) \hat{\chi}^{(j_3j)\varkappa_{j_3}\varkappa_j}_{nk} \rangle \\
&+ \cdots,
\end{aligned} \tag{2.9}$$

where

$$\langle \hat{\chi}^{(ij)\varkappa_i\varkappa_j}_{nk} \rangle = \frac{\delta_{ij}\delta_{\varkappa_i\varkappa_j}}{\omega^2 - \Omega^2_{k\varkappa_i}} \langle \hat{B}^{ii}_{nk} \rangle, \tag{2.10}$$

$$\langle \hat{\chi}^{(ij_2)\varkappa_i\varkappa_{j_2}}_{nk} \hat{\chi}^{(j_1j)\varkappa_{j_1}\varkappa_j}_{nk} \rangle = \frac{\delta_{ij_2}\delta_{\varkappa_i\varkappa_{j_2}}\delta_{j_1j}\delta_{\varkappa_{j_1}\varkappa_j}}{(\omega^2 - \Omega^2_{k\varkappa_i})((\omega^2 - \Omega^2_{k\varkappa_j})} \langle \hat{B}^{ii}_{nk}\ \hat{B}^{jj}_{nk} \rangle. \tag{2.11}$$

Taking into account the fact that $\langle \hat{B}^{ii}_{nk} \hat{B}^{jj}_{nk} \rangle = \langle \hat{B}^{ii}_{nk} \rangle \delta_{ij}$, we find that

$$\langle \hat{g}^{(ij)\varkappa_i\varkappa_j}_{nk,nk} \rangle_* = \delta_{ij} \langle \hat{B}^{ii}_{nk} \rangle [(1 - \hat{g}_{ok} J^{ii}_k(nn))^{-1} \hat{g}_{ok}]^{\varkappa_i\varkappa_j}. \tag{2.12}$$

Let us now evaluate J_k. We introduce the matrix $\widetilde{J}_{k'}$ which is calculated without the constraint that ovals with a given site are absent:

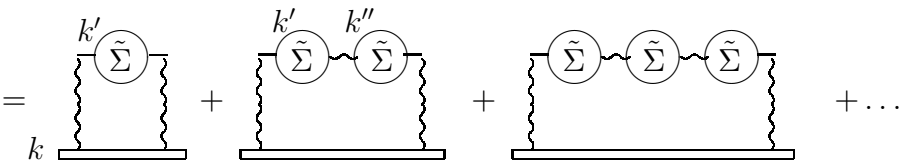

Supposing that $\widetilde{\Sigma}$ may correspond to the initial site as well, we can express $\tilde{J}$ in the form

$$\begin{aligned}
\tilde{J}^{(j_1j_2)\varkappa_{j_1}\varkappa_{j_2}}_{kk}(nn) = \frac{1}{N} \sum_{\mathbf{q}} \Big[\sum_{j'j''} \sum_{\varkappa_{j'}\varkappa_{j''}} \Phi^{(j_1j')\varkappa_{j_1}\varkappa_{j'}}_{kk'}(\mathbf{q})\ \tilde{\Sigma}^{(j'j'')\varkappa_{j'}\varkappa_{j''}}_{k'} \\
\times \Phi^{(j''j_2)\varkappa_{j''}\varkappa_{j_2}}_{k'k}(\mathbf{q}) + (\Phi\ \widetilde{\Sigma}\ \Phi\ \widetilde{\Sigma}\ \Phi)^{(j_1j_2)\varkappa_{j_1}\varkappa_{j_2}}_{kk} + \ldots \Big].
\end{aligned} \tag{2.13}$$

In matrix notations

$$\tilde{J}_k = \frac{1}{N} \sum_{\mathbf{q}} \left[\Phi(\mathbf{q}) \left(1 - \widetilde{\Sigma}\ \Phi(\mathbf{q}) \right)^{-1} \right]_{kk}. \tag{2.14}$$

On the other hand,

$J =$ 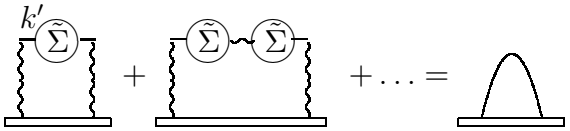 (2.15)

(here $\widetilde{\Sigma}$ does not correspond to the initial site.) Therefore, $\tilde{J}$ can be presented as a series

$\tilde{J} =$ 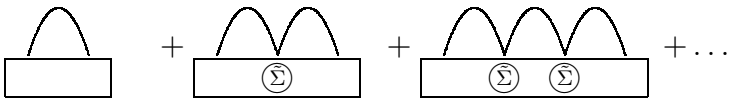

(we use the notations of (2.15), or

$$\tilde{J}_{kk}^{(j_1j_2)\varkappa_{j_1}\varkappa_{j_2}}(nn) = J_{kk}^{(j_1j_2)\varkappa_{j_1}\varkappa_{j_2}}(nn) + \sum_{\substack{j_3j_4\\ \varkappa_{j_3}\varkappa_{j_4}}} J_{kk}^{(j_1j_3)\varkappa_{j_1}\varkappa_{j_3}}(nn)\ \tilde{\Sigma}_k^{(j_3j_4)\varkappa_{j_3}\varkappa_{j_4}}\ J_{kk}^{(j_4j_2)\varkappa_{j_4}\varkappa_{j_2}}(nn)\ + \ldots \tag{2.16}$$

Hence, in a matrix form

$$J_k = (1 + \tilde{J}_k\tilde{\Sigma}_k)^{-1}\tilde{J}_k. \tag{2.17}$$

Let us introduce an auxiliary function

$$\tilde{F}_k = \frac{1}{N}\ \sum_{\mathbf{q}}[\langle\hat{g}\rangle_{\mathbf{q}}^{-1}]_{kk}. \tag{2.18}$$

Then equations (2.14) and (2.17) can be rewritten as

$$J_k = \tilde{\Sigma}_k^{-1} - \tilde{F}_k^{-1}, \tag{2.19}$$

$$\tilde{F}_k = \frac{1}{N}\sum_{\mathbf{q}}\{[\tilde{\Sigma}^{-1} - \Phi(\mathbf{q})]^{-1}\}_{kk}. \tag{2.20}$$

Equations (2.8), (2.12), (2.19) and (2.20) comprise a system of equations for the averaged Green function $\langle\hat{g}\rangle_{\mathbf{q}}$.

3. Calculation of the averaged Green function for a simple model

Let us consider, for example, crystals of the KH_2PO_4 and the CsH_2PO_4 families. Since the frequencies ν_1, ν_2, ν_3, ν_4 of internal vibrations of an isolated PO_4 complex are fairly separated from each other, we can treat the coupled vibrations resulting from modes A_1, E, F_2, F_2 independently. The $\varkappa_i$ takes only one value ($p_k = 1$) in the case of A_1 mode, two values ($p_k = 2$) in the case of E mode and three values ($p_k = 3$) in the cases of F_2 modes.

Let us consider, as an example, the case of A_1 mode. We restrict our consideration to a simple model. We assume that there is only one group PO_4 per unit cell ($k = 1$), and only two proton configurations around this group are allowed ($r = 2$). Configurations with protons close to upper or lower oxygen atoms (with respect to the c-axis of the crystal) (the case $i = 1, 2$ [9,10]) have the lowest energy. Then, $\widetilde{\Sigma_k} = \widetilde{\Sigma}$, and

$$\widetilde{\Sigma}^{-1} = \langle \hat{g} \rangle_*^{-1} + J \ . \tag{3.1}$$

Let us denote the diagonal elements of the matrices J and $\Phi(\mathbf{q})$ as J_{11} and $\Phi_{11}(\mathbf{q})$, respectively, and their non-diagonal elements as J_{12} and $\Phi_{12}(\mathbf{q})$. Equations (2.8), (2.12), (2.19), (2.20) are transformed into the system of equations

$$\tilde{\Sigma} = \frac{\tilde{g}}{D} \begin{pmatrix} 1 + \tilde{g}(J_{11} - J_{12}) & 0 \\ 0 & 1 + \tilde{g}(J_{11} + J_{12}) \end{pmatrix}, \tag{3.2a}$$

$$\langle \hat{g} \rangle_* = \begin{pmatrix} \tilde{g} & 0 \\ 0 & \tilde{g} \end{pmatrix}, \quad \tilde{g} = \langle B^{11} \rangle (1 - g_0 J_{11})^{-1} g_0, \tag{3.2b}$$

$$\begin{aligned} \tilde{F} &= \begin{pmatrix} F + F' & 0 \\ 0 & F - F' \end{pmatrix} \\ &= \frac{1}{N} \sum_{\mathbf{q}} \begin{pmatrix} \tilde{g}^{-1} + (J_{11} + J_{12}) - (\Phi_{11}(\mathbf{q}) + \Phi_{12}(\mathbf{q})) & 0 \\ 0 & \tilde{g}^{-1} - (J_{11} - J_{12}) - (\Phi_{11}(\mathbf{q}) - \Phi_{12}(\mathbf{q})) \end{pmatrix}, \end{aligned} \tag{3.2c}$$

$$\begin{aligned} J = \begin{pmatrix} J_{11} + J_{12} & 0 \\ 0 & J_{11} - J_{12} \end{pmatrix} = \begin{pmatrix} \tilde{g}^{-1} + J_{11} + J_{12} & 0 \\ 0 & \tilde{g}^{-1} + J_{11} - J_{12} \end{pmatrix} - \\ - \begin{pmatrix} F + F' & 0 \\ 0 & F - F' \end{pmatrix}^{-1}, \end{aligned} \tag{3.2d}$$

where

$$D = (1 + \tilde{g} J_{11})^2 - (\tilde{g} J_{12})^2. \tag{3.3}$$

From (3.2c) we get

$$\tilde{g} = \frac{1}{N} \sum_{\mathbf{q}} \frac{1}{(\tilde{g}^{-1} + J_{11} - \Phi_{11}(\mathbf{q})) \mp (J_{12} - \Phi_{12}(\mathbf{q}))}. \tag{3.4}$$

Within an isotropic crystal approximation, we take $\Phi_{12}(\mathbf{q}) = \Phi_0'/\Phi_0 \Phi_{11}(\mathbf{q})$. Replacing the sum in (3.4) by an integral with a half-elliptic density of states,

$$\rho(t) = \frac{2}{\pi \Phi_0^2} \sqrt{\Phi_0^2 - t^2}, \tag{3.5}$$

we get the following expressions for the elements of matrix J:

$$J_{11} = \frac{1}{2} g_0^{-1} \Big[1 - \sqrt{1 - g_0^{-1} (\Phi_0^2 + \Phi_0'^2) \langle B \rangle} \Big], \tag{3.6}$$

$$J_{12} = g_0^{-1} \frac{\Phi_0 \Phi_0'}{\Phi_0^2 + \Phi_0'^2} \Big[1 - \sqrt{1 - g_0^{-1} (\Phi_0^2 + \Phi_0'^2) \langle B \rangle} \Big]. \tag{3.7}$$

Here we take into account the fact that $\langle B^{11}\rangle = \langle B^{22}\rangle = \langle B\rangle$, which corresponds to temperatures above T_c.

Let us consider now the Green function (2.4) built on polarizability operators. Since the wave vector hardly changes at the Raman scattering, we assume that $\mathbf{q} \approx 0$. As one can see from (2.1), the effective cross-section of the Raman scattering is proportional to the imaginary part of the Green function $\langle\hat{G}\rangle$. Using relation (2.4) we find that

$$\begin{aligned}\mathrm{Im}\langle\hat{G}\rangle_{\mathbf{q}=0} = \mathrm{Im}[&\mathbf{R}^{(1)}\mathbf{R}^{*(1)}\langle q\rangle^{11}_{\mathbf{q}=0} + \mathbf{R}^{(1)}\mathbf{R}^{*(2)}\langle q\rangle^{12}_{\mathbf{q}=0} \\ &+\mathbf{R}^{(2)}\mathbf{R}^{*(1)}\langle q\rangle^{21}_{\mathbf{q}=0} + \mathbf{R}^{(2)}\mathbf{R}^{*(2)}\langle q\rangle^{22}_{\mathbf{q}=0}]\end{aligned} \tag{3.8}$$

for the model under consideration. As one can easily show,

$$\langle q\rangle^{11}_{\mathbf{q}=0} = \frac{1}{2}\Big(\frac{1}{A+C} + \frac{1}{A-C}\Big), \tag{3.9}$$

$$\langle q\rangle^{12}_{\mathbf{q}=0} = \frac{1}{2}\Big(\frac{1}{A+C} - \frac{1}{A-C}\Big), \tag{3.10}$$

here A and C are elements of the matrix $\langle\hat{g}\rangle^{-1}$

$$\langle\hat{g}\rangle^{-1} = \begin{pmatrix} A & C \\ C & A \end{pmatrix}.$$

Making use of (3.9) and (3.10) and taking into account the tensor symmetry which corresponds to the point symmetry of a crystal, we can write Im $\langle\hat{G}\rangle_{\mathbf{q}=0}$ as for a KH_2PO_4 crystal [9,10]:

(zz)-scattering

$$\mathrm{Im}\langle\hat{G}\rangle_{\mathbf{q}=0} = 2|g_3|^2\mathrm{Im}\frac{1}{A+C}; \tag{3.11}$$

(xy)-scattering

$$\mathrm{Im}\langle\hat{G}\rangle_{\mathbf{q}=0} = 2|h|^2\mathrm{Im}\frac{1}{A-C}; \tag{3.12}$$

(xx) and (yy)-scattering

$$\begin{aligned}\mathrm{Im}\langle\hat{G}\rangle_{\mathbf{q}=0} = &\Big[\frac{1}{2}\Big(|g_1|^2 + |g_2|^2\Big) + g_1^{'}g_2^{'} + g_1^{''}g_2^{''}\Big]\mathrm{Im}\frac{1}{A+C} \\ &+ \Big[\frac{1}{2}\Big(|g_1|^2 + |g_2|^2\Big) - g_1^{'}g_2^{'} - g_1^{''}g_2^{''}\Big]\mathrm{Im}\frac{1}{A-C}.\end{aligned} \tag{3.13}$$

for a quasi one-dimensional CsH_2PO_4 crystal[1]

(xx)-scattering

$$\mathrm{Im}\langle\hat{G}\rangle_{\mathbf{q}=0} = 2|c_{11}^{'}|^2\mathrm{Im}\frac{1}{A+C}; \tag{3.14}$$

[1]Symmetry analysis of the Raman scattering from the CsH_2PO_4-type crystal when the configurational splitting is taken into account is given in the Appendix

(analogous expressions were also obtained for (yy), (zz), (xz)-scattering, with different coefficients).

(xy)-scattering

$$\mathrm{Im}\langle\hat{G}\rangle_{\mathbf{q}=0} = 2|c_{12}^{'}|^2\mathrm{Im}\frac{1}{A-C}. \tag{3.15}$$

A similar, but with a different coefficient, expression was obtained for the case of (yz)-scattering.

Expressions (3.11)-(3.15) contain not only the quantities Im $1/(A+C)$ and Im $1/(A-C)$ but also the elements of the scattering tensor as "weight" factors defining the contribution of each item. Let us consider, for instance, $1/(A+C)$. With the help of (3.1), (3.6) and (3.7) we can rewrite its imaginary part as

$$\begin{aligned}\mathrm{Im}\frac{1}{A+C} = &-\Big(\frac{1}{2} - \frac{\Phi_0\Phi_0^{'}}{\Phi_0^2+\Phi_0^{'2}}\Big)\sqrt{\frac{1}{2}(\Phi_0^2+\Phi_0^{'2}) - (\omega^2-\Omega^2)^2} \\ &\times\Big[\Big(\frac{3}{2} + \frac{\Phi_0\Phi_0^{'}}{\Phi_0^2+\Phi_0^{'2}}\Big)(\omega^2-\Omega^2) - \Phi_0 - \Phi_0^{'}\Big]^2 \\ &+ \Big(\frac{1}{2} - \frac{\Phi_0\Phi_0^{'}}{\Phi_0^2+\Phi_0^{'2}}\Big)^2\Big[\frac{1}{2}(\Phi_0^2+\Phi_0^{'2}) - (\omega^2-\Omega^2)^2\Big]^{-1}.\end{aligned} \tag{3.16}$$

For $1/(A-C)$ we have

$$\begin{aligned}\mathrm{Im}\frac{1}{A-C} = &-\Big(\frac{1}{2} + \frac{\Phi_0\Phi_0^{'}}{\Phi_0^2+\Phi_0^{'2}}\Big)\sqrt{\frac{1}{2}\ (\Phi_0^2+\Phi_0^{'2}) - (\omega^2-\Omega^2)^2} \\ &\times\Big[\Big(\frac{3}{2} - \frac{\Phi_0\Phi_0^{'}}{\Phi_0^2+\Phi_0^{'2}}\Big)(\omega^2-\Omega^2) - \Phi_0 + \Phi_0^{'}\Big]^2 \\ &+ \Big(\frac{1}{2} + \frac{\Phi_0\Phi_0^{'}}{\Phi_0^2+\Phi_0^{'2}}\Big)^2\Big[\frac{1}{2}(\Phi_0^2+\Phi_0^{'2}) - (\omega^2-\Omega^2)^2\Big]^{-1}.\end{aligned} \tag{3.17}$$

The region where the imaginary parts differ from zero is defined by the inequalities

$$\omega_{\mathrm{lim}(2)} < \omega < \omega_{\mathrm{lim}(1)}$$

where

$$\omega_{\mathrm{lim}(1,2)} = \sqrt{\Omega^2 \pm \sqrt{\frac{1}{2}(\Phi_0^2+\Phi_0^{'2})}}. \tag{3.18}$$

As numerical calculations show, functions (3.16) and (3.17) have sharp peaks in the vicinity of $\omega_{\mathrm{lim}(1)}$. In this region the imaginary part of $1/(A+C)$ can be approximated as

$$\mathrm{Im}\frac{1}{A+C} = \frac{az}{a_1+a_2z^2}, \tag{3.19}$$

where $z = \sqrt{\omega_{\mathrm{lim}(1)}^2 - \omega^2}$ is small. The coefficients a, a_1, a_2 are expressed in terms of the energies of interactions between internal vibrations of PO_4 groups having different configurations.

Using formula (3.19) and an analogous to it one for Im $1/(A-C)$ with the coefficients a', a'_1, a'_2, we can determine the values of the ratio

$$\xi = \Phi'_0 \Big/ \Phi_0, \tag{3.20}$$

for which the maxima of the quantities

$$f_1(\xi) = \Big(\mathrm{Im}\frac{1}{A+C}\Big)_{\max}, \tag{3.21}$$

$$f_2(\xi) = \Big(\mathrm{Im}\frac{1}{A-C}\Big)_{\max}, \tag{3.22}$$

occurring in the expressions of the averaged Green function $\langle\hat{G}\rangle$ are of the same order of magnitude. The obtained dependencies are shown in figure 1. As one can see, the values of Im $1/(A\pm C)$ maxima slightly differ only at small values of ξ.

The distance between the peaks is determined by the difference between frequencies corresponding to the maxima of Im $1/(A+C)$ and Im $1/(A-C)$

$$\Delta\omega = \Big(\Omega^2 + \Phi_0\sqrt{\frac{1}{2}(1+\xi^2)} - \frac{a_1}{a_2}\Big)^{1/2} - \Big(\Omega^2 + \Phi_0\sqrt{\frac{1}{2}(1+\xi^2)} - \frac{a'_1}{a'_2}\Big)^{1/2}. \tag{3.23}$$

Frequency separation (3.23) depends on absolute values of the energies of interaction between equal and different configurational types of PO_4 groups.

In figures 2a and 2b we plot the curves for Im $1/(A\pm C)$. The parameters values are chosen allowing for the condition of comparability of functions (3.21) and (3.22) and the condition of sufficient separation $\Delta\omega$ of scattering peaks too.

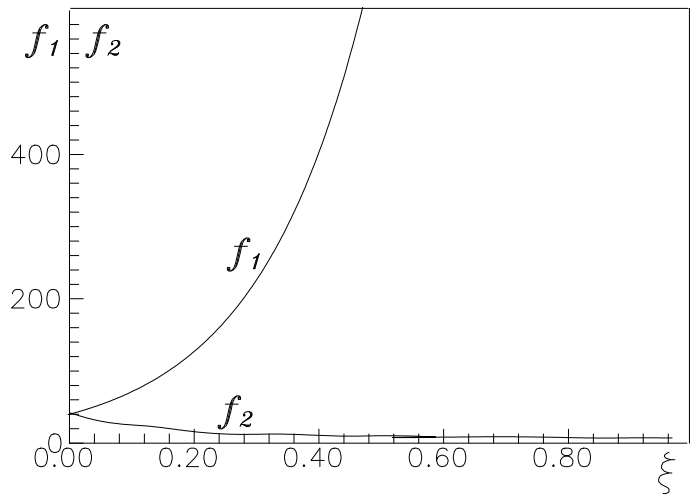

Figure 1. Dependence of the functions $f_1 = (\mathrm{Im}\ 1/(A+C))_{\max}$ and $f_2 = (\mathrm{Im}\ 1/(A-C))_{\max}$ defined the Raman scattering intensity for different geometries on constants of interaction of ion complexes internal vibrations.

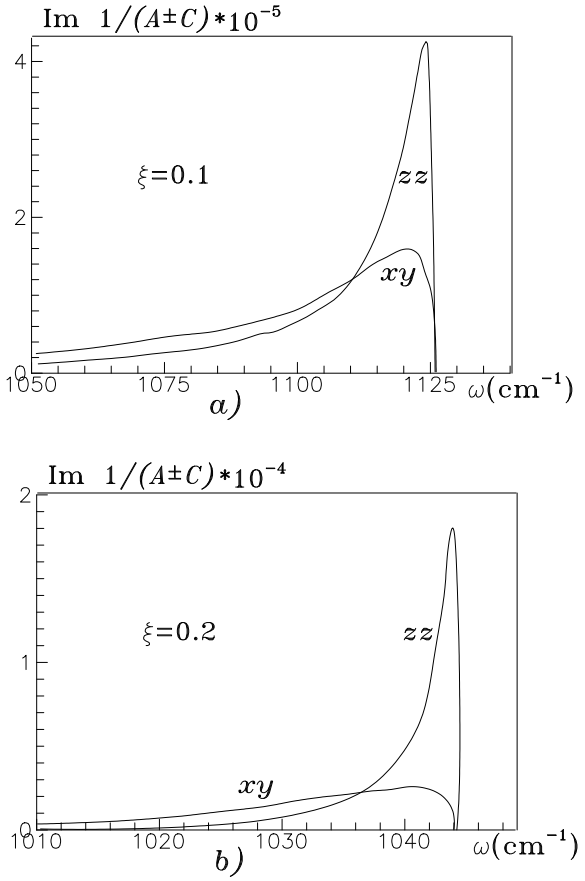

Figure 2. Configurational splitting in the Raman spectrum for the CDP crystal model for different constants of ion complexes internal vibrations.

4. Discussion

The results obtained for a simple model confirm the possibility of configurational splitting which manifests itself as additional lines of Raman spectra at $T > T_c$.

Depending on the scattering geometry, one or two split components may appear in the spectrum. In the former case, scattering in different geometries can be observed at different frequencies, that is some frequency shift takes place.

To observe two lines in the case when they can appear simultaneously (for instance (3.13)), a sufficient frequency separation determined by (3.23) is necessary. Besides, as well as in the case of one component, these two lines must be intensive enough, which depends on absolute values of scattering tensor elements $\mathbf{R}_{l\alpha\beta}^{(i)\varkappa_i}$.

As follows from the above analysis, the corresponding lines of Raman spectra may be of different width and intensity and can be observed in different scattering geometries. Simultaneous observation of split components is possible only at certain relations among the constants of interactions among various ion group configurations.

The proposed method of the calculation of spectral density functions which determine line profiles in Raman spectra can also be applied to more sophisticated models.

Appendix

By means of structural and dielectric studies, the symmetry of the paraelectric CsH_2PO_4 (CDP) crystal was found to be monoclinic (the space group C_{2h}^2 [16]). The crystal structure of CDP essentially differs from that of KDP, mainly by the H-bond network configuration, positions of Cs^+ ions and the order of PO_4^{3-} groups along the polar axis. Depending on the nature of the protons positions on hydrogen bonds, different configurations of H_nPO_4 groups ($n = 1, 2, 3$) can be realized. Among them the configurations presented in figure 1 are most probable.

The electronic spectrum of PO_4 groups is most sensitive to the positions of the nearest protons. Therefore, the scattering tensors $\mathbf{R}_{l\alpha\beta}^{(j)\varkappa_j}$ are different for different H_nPO_4 configurations. The symmetry analysis allows one to elucidate the structure of these tensors for all the considered configurations (see figure A.1). Amongst the $\mathbf{R}_{l\alpha\beta}^{(j)\varkappa_j}$ tensors components, the ones which describe scattering in the case of the isolated complexes of T_d symmetry and those allowed by the local symmetry C_{1h} must be the largest.

The presence of lines ν_i in Raman spectra of the given scattering geometry is determined by the structure of $\mathbf{R}_{l\alpha\beta}^{(i)\varkappa_i}$ tensors, as well as by the symmetry of coupled vibrations. The geometry of the scattering of modes coming from different PO_4 configurations at $T > T_c$ is given in table A.1.

Internal vibrations of an isolated PO_4 complex (point symmetry T_d) are classified by irreducible representations A_1 (frequency ν_1), E (frequency ν_2), and F_2 (frequencies ν_3 and ν_4). In a crystal they transform into the modes of symmetries A_g; A_g, B_g; A_g, A_g, B_g in the case of $i = 1$ ($l = 1$) and $i = 5$ ($l = 2$) configurations, A_g, B_g; A_g, B_g, A_g, B_g; A_g, B_g, A_g, B_g, A_g, B_g in the case of $i = 2, 3$ ($l = 1$) and $i = 6, 7$ ($l = 2$) configurations, and A_g; A_g, B_g; A_g, A_g, B_g in the case of $i = 4$ ($l = 1$) and $i = 8$ ($l = 2$) configurations, respectively.

Since the symmetry of H_nPO_4 ($n = 1, 2, 3$) configurations is lower than C_{1h} of PO_4 groups, in some instances there may appear the lines forbidden by both the site symmetry and configurational splitting.

In particular, such a situation takes place in (xz) scattering (the z-axis is directed along the chain of H-bonds on which protons are ordered at all temperatures; the y-axis coincides with the polar axis, and $x \perp yz$). From table A.1 it follows that mode ν_2 of A_g symmetry may split[1]. Such a splitting is not allowed by the local symmetry C_{1h}; moreover, in the case of T_d symmetry this mode is forbidden at all. These results confirm the experiment [11]. The observed split lines are of approximately equal(insignificant) intensity, the splitting itself is of about 83 cm^{-1}.

[1]The frequencies values are given in [17]

Configurational splitting may also take place in (xy)-scattering (frequencies ν_2 and ν_4 of A_g and B_g symmetries), (yz)-scattering (frequency ν_4 of B_g symmetry), (xx), (yy), (zz), (xz)-scattering (frequency ν_4 of A_g symmetry). The two former cases have been studied experimentally [18].

Table A.1 also describes the situation when, in addition to splitting, the appearance of lines forbidden by the site symmetry is possible. It is found out that in addition to ν_2, ν_3 and ν_4 frequencies, line ν_1 of B_g symmetry may appear in the (xy) and (yz) spectra. However, in [18] neither the ν_1 line in the scattering of this geometry nor the splitting of the ν_4 mode in (xx), (yy), (zz), (xz)-scattering was observed. We may attribute that to a low intensity of the expected lines, for they originate from the $i = 2, 3, 6, 7$ configurations only.

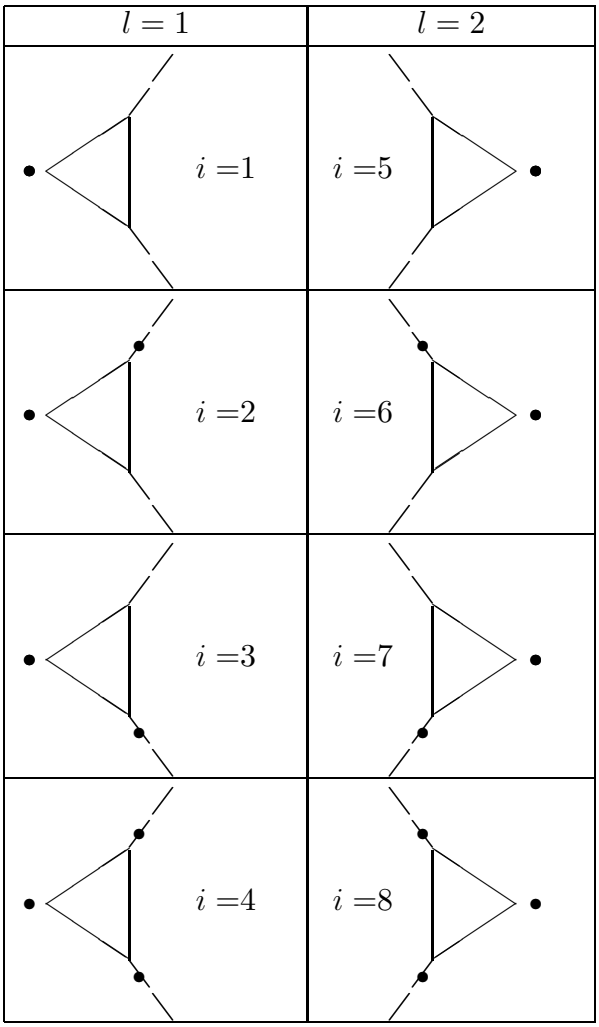

Figure A.1. The H_nPO_4 configurations $(n = 1, 2, 3)$ for two sublattices of PO_4 groups in a CsH_2PO_4 crystal; projection on the xy-plane.

C_{1h}	T_d	C_{2h}	$\mathbf{R}_{xx}$	$\mathbf{R}_{yy}$	$\mathbf{R}_{zz}$	$\mathbf{R}_{xy}$	$\mathbf{R}_{xz}$	$\mathbf{R}_{yz}$	configurations 1, 5	configurations 2, 3, 6, 7	configurations 4, 8
(A')	$\boxed{A_1}$	$3A_g$	$\boxed{\circledast}$	$\boxed{\circledast}$	$\boxed{\circledast}$		$\circledast$		A_g	A_g	A_g
		B_g				$*$		$*$		B_g	
		A_u								A_u	
		$3B_u$							B_u	B_u	B_u
(A'')	$\boxed{F_2}$	A_g	$*$	$*$	$*$		$*$			A_g	
		$3B_g$				$\boxed{\circledast}$		$\circledast$	B_g	B_g	B_g
		$3A_u$							A_u	A_u	A_u
		B_u								B_u	
(A')	$\boxed{F_2}$	$3A_g$	$\circledast$	$\circledast$	$\circledast$		$\boxed{\circledast}$		A_g	A_g	A_g
		B_g				$*$		$*$		B_g	
		A_u								A_u	
		$3B_u$							B_u	B_u	B_u
(A')	$\boxed{F_2}$	$3A_g$	$\circledast$	$\boxed{\circledast}$	$\boxed{\circledast}$		$\circledast$		A_g	A_g	A_g
		B_g				$*$		$*$		B_g	
		A_u								A_u	
		$3B_u$							B_u	B_u	B_u
(A')	$\boxed{E}$	$3A_g$	$\boxed{\circledast}$	$\boxed{\circledast}$	$\boxed{\circledast}$		$\circledast$		A_g	A_g	A_g
		B_g				$*$		$\boxed{*}$		B_g	
		A_u								A_u	
		$3B_u$							B_u	B_u	B_u
(A'')	$\boxed{E}$	A_g	$\boxed{*}$	$\boxed{*}$	$\boxed{*}$		$*$			A_g	
		$3B_g$				$\circledast$		$\boxed{\circledast}$	B_g	B_g	B_g
		$3A_u$							A_u	A_u	A_u
		B_u								B_u	

Table A.1. Geometry of the scattering of configurationally split modes of the CsH_2PO_4 crystal; $T > T_c$. First column – irreducible representations of a site PO_4 group symmetry. Second column – irreducible representations of an isolated PO_4 group. Third column – configurational splitting. Symbols $*$ denote non-zero components of scattering tensors; $\boxed{*}$ corresponds to the scattering of isolated complexes PO_4; $\circledast$ stands for the scattering allowed by a site C_{1h} symmetries. Three last columns contain symmetry of the modes arising from different configurations.

i=1

$\varkappa_i = (1|F_2)$

	a_{12}	
a_{12}		a_{23}
	a_{23}	

$\varkappa_i = (2|F_2)$

a_{11}		a_{13}
	a_{22}	
a_{13}		a_{33}

$\varkappa_i = (3|F_2)$

b_{11}		b_{13}
	b_{22}	
b_{13}		b_{33}

(A_1)

c_{11}		c_{13}
	c_{22}	
c_{13}		c_{33}

$(1|E)$

d_{11}		d_{13}
	d_{22}	
d_{13}		d_{33}

$(2|E)$

	d_{12}	
d_{12}		d_{23}
	d_{23}	

i=2

$(1|F_2)$

$a'_{11}+a''_{11}$	$a'_{12}+a''_{12}$	$a'_{13}+a''_{13}$
$a'_{12}+a''_{12}$	$a'_{22}+a''_{22}$	$a'_{23}+a''_{23}$
$a'_{13}+a''_{13}$	$a'_{23}+a''_{23}$	$a'_{33}+a''_{33}$

$(2|F_2)$

$a'_{11}-a''_{11}$	$a'_{12}-a''_{12}$	$a'_{13}-a''_{13}$
$a'_{12}-a''_{12}$	$a'_{22}-a''_{22}$	$a'_{23}-a''_{23}$
$a'_{13}-a''_{13}$	$a'_{23}-a''_{23}$	$a'_{33}-a''_{33}$

$(3|F_2)$

b'_{11}	b'_{12}	b'_{13}
b'_{12}	b'_{22}	b'_{23}
b'_{13}	b'_{23}	b'_{33}

(A_1)

c'_{11}	c'_{12}	c'_{13}
c'_{12}	c'_{22}	c'_{23}
c'_{13}	c'_{23}	c'_{33}

$(1|E)$

$d'_{11}+d''_{11}$	$d'_{12}+d''_{12}$	$d'_{13}+d''_{13}$
$d'_{12}+d''_{12}$	$d'_{22}+d''_{22}$	$d'_{23}+d''_{23}$
$d'_{13}+d''_{13}$	$d'_{23}+d''_{23}$	$d'_{33}+d''_{33}$

$(2|E)$

$d'_{11}-d''_{11}$	$d'_{12}-d''_{12}$	$d'_{13}-d''_{13}$
$d'_{12}-d''_{12}$	$d'_{22}-d''_{22}$	$d'_{23}-d''_{23}$
$d'_{13}-d''_{13}$	$d'_{23}-d''_{23}$	$d'_{33}-d''_{33}$

i=3

$(1|F_2)$

$a'_{11}+a''_{11}$	$-a'_{12}-a''_{12}$	$a'_{13}+a''_{13}$
$-a'_{12}-a''_{12}$	$a'_{22}+a''_{22}$	$-a'_{23}-a''_{23}$
$a'_{13}+a''_{13}$	$-a'_{23}-a''_{23}$	$a'_{33}+a''_{33}$

$(2|F_2)$

$a'_{11}-a''_{11}$	$-a'_{12}+a''_{12}$	$a'_{13}-a''_{13}$
$-a'_{12}+a''_{12}$	$a'_{22}-a''_{22}$	$-a'_{23}+a''_{23}$
$a'_{13}-a''_{13}$	$-a'_{23}+a''_{23}$	$a'_{33}-a''_{33}$

$(3|F_2)$

b'_{11}	$-b'_{12}$	b'_{13}
$-b'_{12}$	b'_{22}	$-b'_{23}$
b'_{13}	$-b'_{23}$	b'_{33}

(A_1)

c'_{11}	$-c'_{12}$	c'_{13}
$-c'_{12}$	c'_{22}	$-c'_{23}$
c'_{13}	$-c'_{23}$	c'_{33}

$(1|E)$

$\overline{(d'_{11}+d''_{11})}$	$-d'_{12}-d''_{12}$	$\overline{(d'_{13}+d''_{13})}$
$-d'_{12}-d''_{12}$	$\overline{(d'_{22}+d''_{22})}$	$-d'_{23}-d''_{23}$
$\overline{(d'_{13}+d''_{13})}$	$-d'_{23}-d''_{23}$	$\overline{(d'_{33}+d''_{33})}$

$(2|E)$

$d'_{11}-d''_{11}$	$\overline{(-d'_{12}+d''_{12})}$	$d'_{13}-d''_{13}$
$\overline{(-d'_{12}+d''_{12})}$	$d'_{22}-d''_{22}$	$\overline{(-d'_{23}+d''_{23})}$
$d'_{13}-d''_{13}$	$\overline{(-d'_{23}+d''_{23})}$	$d'_{33}-d''_{33}$

Figure A.2. Structure of scattering tensors $\mathbf{R}^{(i)\varkappa_i}_{l\alpha\beta}$. By rectangles and ovals we denote components allowed by the symmetry T_d and the site symmetry C_{1h}, respectively.

References

1. Blinc R., Zeks B. Dynamics of order-disorder-type ferroelectrics and antiferroelectrics. // Adv. Phys., 1972, vol. 21, p. 693–757.
2. Bruce A.D. Cowley R.A. Structural phase transition. III. Critical dynamics and quasi-elastic scattering. // Adv. Phys., 1980, vol. 29, No. 1, p. 219–321.
3. Tominaga Y., Urabe H., Tokunaga M. Internal modes and local symmetry of PO_4 tetrahedrons in KH_2PO_4 by Raman scattering. // Solid State Commun., 1983, vol. 48, No. 3, p. 265–267.
4. Tanaka H., Tokunaga M., Tatsuzaki I. Internal modes and the local symmetry of PO_4 tetrahedra in $K(H_{1-x}D_x)_2PO_4$ by Raman scattering. // Solid State Commun., 1984, vol. 49, No. 2, p. 153–155.
5. Tokunaga M. Order-disorder model of PO_4-dipoles for KH_2PO_4 type ferroelectric phase transition. // Progr. Theor. Phys. Suppl., 1984, No. 80, p. 156–162.
6. Tominaga Y., Tokunaga M., Tatsuzaki I. Dynamical mechanism of ferroelectric phase transition in KH_2PO_4 by Raman scattering study. // Jap. J. Appl. Phys., 1985, Pt. 1, vol. 24, Suppl. 24–2, p. 917–919.
7. Tokunaga M., Tatsuzaki I. Light scattering spectra of polarization fluctuation and models of the phase transition in KDP type ferroelectrics. // Phase Transition, 1984, vol. 4, No. 1, p. 97–156.
8. Tokunaga M., Tominaga Y., Tatsuzaki I. Order-disorder model of PO_4 dipoles in KDP based on recent Raman spectroscopic studies. // Ferroelectrics, 1985, vol. 63, No. 1/4, p. 171–178.
9. Blinc R. 170 NQR and the mechanism of the phase transition in KH_2PO_4 type H-bonded systems. // Z. Naturforsch., 1986, vol. 41a, p. 249–255.
10. Stasyuk I.V., Ivankiv Ya.L. Raman light scattering in crystals with ordered structure elements. // Preprint ITP–87–57R (Kyiv, 1987), 25 p. (in Russian).
11. Levitskii R.R., Sorokov S.I., Sokolovskii R.O. Correlations functions of quenched and annealed Ising systems. // Cond. Matt. Phys., 1995, No. 5, p. 81–104.
12. Cowley R.A. The lattice dynamics of an anharmonic crystal. // Adv. Phys., 1963, vol. 12, No. 48, p. 421–481.
13. Cardona M. Introduction. In: "Light scattering in Solids". Ed. by M.Cardona, Berlin-Heidelberg-New York, Springer-Verlag, 1975, p. 11–37.
14. Elliot R.J., Krumhansl J.A., Leath P.L. Theory and properties of randomly disordered

crystals and related physical systems. // Rev. Mod. Phys., 1974, vol. 46, p. 465–702.
15. Stasyuk I.V., Ivankiv Ya.L. Dynamic susceptibility of systems described by de Gennes model. In: Spectroscopy of Molecules and Crystals., Pt. 2, Kyiv, Naukova dumka, 1980, p. 176–179.
16. Uesu Y., Kobayashi J. Crystal structure and ferroelectricity of cesium dihydrogen phosphate // Phys. Status Solidi (a), 1976, vol. 34, No. 2, p. 475–481.
17. Martinez J.L., Calleja J.M., Gonzalo J.A. Temperature dependence of internal modes and local symmetry of PO_4 tetrahedra in RbH_2PO_4 (RDP) and RbD_2PO_4 (DRDP) by Raman scattering. // Solid State Commun., 1984, vol. 52, No. 5, p. 499–501.
18. Kasahara M., Aoki M., Tatsuzaki I. Raman study of the phase transition in CsH_2PO_4 and CsD_2PO_4. // Ferroelectrics, 1984, vol. 55, No. 1–4, p. 715–718.

Конфігураційне розщеплення в раманівських спектрах у кристалах з фазовими переходами типу лад-безлад

І.В.Стасюк, Я.Л.Іванків

Інститут фізики конденсованих систем НАН України,
290011 Львів, вул. Свєнціцького, 1

Отримано 23 червня 1997

В наближенні когерентного потенціалу одержана система рівнянь для усередненої фононної функції Гріна, що визначає профілі ліній в спектрах Рамана. На прикладі простої моделі проведено дослідження конфігураційно розщеплених компонент раманівських ліній. Для сегнетоелектриків типу KH_2PO_4 та CsH_2PO_4 обговорюється питання про можливий експериментальний вияв конфігураційного розщеплення.

Ключові слова: *комбінаційне розсіяння, конфігураційне розщеплення, фазові переходи типу лад-безлад, сегнетоелектрики*

PACS: *77.84.Fa, 78.30.Ly*